Coupled Systems Mechanics, *Vol. 9, No. 4 (2020) 311-323*
DOI: https://doi.org/10.12989/csm.2020.9.4.311

Effective mode shapes of multi-storey frames subjected to moving train loads

Salih Demirtaş* and Hasan Ozturk[a]

Department of Mechanical Engineering, Dokuz Eylul University, 35397, Buca, İzmir, Turkey

(Received December 30, 2019, Revised February 27, 2020, Accepted February 28, 2020)

Abstract. This paper deals with the effect of the mode shapes on the dynamic response of a multi-storey frame subjected to moving train loads which are modelled as loads of constant intervals with constant velocity using the finite element method. The multi-storey frame is modelled as a number of Bernoulli-Euler beam elements. First, the first few modes of the multi-storey frame are determined. Then, the effects of force span length to beam length ratio and velocity on dynamic magnification factor (DMF) are evaluated via 3D velocity-force span length to beam length ratio-DMF graphics and its 2D projections. By using 3D and 2D graphics, the directions of critical speeds that force the structure under resonance conditions are determined. Last, the mode shapes related to these directions are determined by the time history and frequency response graphs. This study has been limited by the vibration of the frame in the vertical direction.

Keywords: multi-storey frame; moving force; the finite element method; dynamic magnification factor; mode shape

1. Introduction

Dynamic responses of engineering structures under the action of moving loads, such as bridges, gantry cranes, conveyor systems, etc., have seen considerable interests over the years. Fryba (1999) have presented various analytic methods for predicting the dynamic behaviour of simple and continuous beams under moving loads in his classical monograph. Thambiratnam and Zhuge (1996) have presented a study for determining the effects of some parameters, such as the foundation stiffness, travelling speed, length of beam and stiffness of the sprung mass, on the dynamic responses of beams under a concentrated moving load. Wu *et al.* (2000) have calculated the equivalent nodal forces and moments to represent the moving loads by using three approximate methods. In the first "full" method, equivalent nodal forces and moments have been calculated. This requires the shape functions for the elements. The second method simply ignores the moments calculated using method 1. The third "simple" method ignores any moments applied at the nodes at the outset and therefore does not require knowledge of the shape functions. Kıral and Kıral (2007) have investigated dynamic responses of a symmetric laminated composite beam under a concentrated force with a constant velocity. Wu *et al.* (2001) have developed a technique for obtaining the response of three-

*Corresponding author, Ph.D., E-mail: salih.demirtas@deu.edu.tr
[a]Professor, E-mail: hasan.ozturk@deu.edu.tr

http://www.techno-press.org/?journal=csm&subpage=8 ISSN: 2234-2184 (Print), 2234-2192 (Online)

dimensional structures to the movement of bodies in two dimensions on their surface. Fu (2015) has investigated the effect of cracks on the vibration behaviour of a continuous beam bridge under the moving vehicle. Zrnić *et al.* (2015) have investigated dynamic responses of a gantry crane system subjected to an elastically suspended moving body using a combined finite element and analytical method. Ozturk *et al.* (2015) have studied the effects of crack depth and crack location on the in-plane static and dynamic stability of cracked multi-bay frame structures subjected to periodic loading using the finite element method. Koziol (2016) has presented a wavelet-based semi-analytical solution for the infinite Euler-Bernoulli beam resting on a nonlinear foundation subjected to a set of moving force. Mohebpour *et al.* (2016) have used a finite element method based on the classical lamination theory to study the dynamic response of an inclined cross-ply laminated composite beam under moving mass. Song *et al.* (2016) have proposed a frequency domain spectral element method (SEM) for a Timoshenko beam model subjected to a moving point force. Svedholm *et al.* (2016) have investigated the dynamic behaviour of a non-proportionally damped Euler-Bernoulli beam with general end conditions under a moving load.

Frame structures, for instance, gantry crane and bridges, having the combination of beams and columns, subjected to moving force are often encountered in engineering applications. Zrnić *et al.* (2015) have modelled a gantry crane system as a 1-storey frame. Yang *et al.* (2004) have studied resonance and cancellation phenomena in the train induced vibrations of railway bridges with elastic bearings. If the elastic support is considered as a column, railway bridges with elastic bearings can be modelled as a 1-storey frame.

In this study, the case where the concentrated load speed takes small values can be considered as a gantry crane, and the case of high-speed values of successive moving force with constant interval can be considered as a train induced vibration of railway bridges. In addition, the structure having more than one storeys is also examined.

The dynamic responses of a multi-storey frame under the action of moving train loads have been investigated by using the finite element method in this study. The train loads are modelled as loads of constant intervals with constant velocity. It is assumed that the boundary conditions of the frame are zero horizontal and vertical displacements and zero rotations at bases of columns. The main aspects of this paper are as follows:

- The effect of the load velocity and force span length to beam length ratio on the dynamic magnification factor (DMF) has been studied by means of the 3D velocity-force span length to beam length ratio-DMF plots.
- The effect of mode shapes of the multi-storey frame on the dynamic response of a multi-storey frame has been investigated.
- The dominant mode shapes of the resonance vibrations in the vertical direction have been determined.

2. Description of the numerical model and finite element formulation

2.1 Description of the numerical model

The system considered, shown schematically in Fig. 1, is a multi-storey frame subjected to train moving forces having a magnitude of F with a constant velocity of V. The Bernoulli-Euler beam theory is used in the analysis. It is assumed that beams and columns have length L, elastic modulus E, mass per unit length m, area moment of inertia I, cross-section area A, respectively. The distance between successive loads is the same and denoted as L_f.

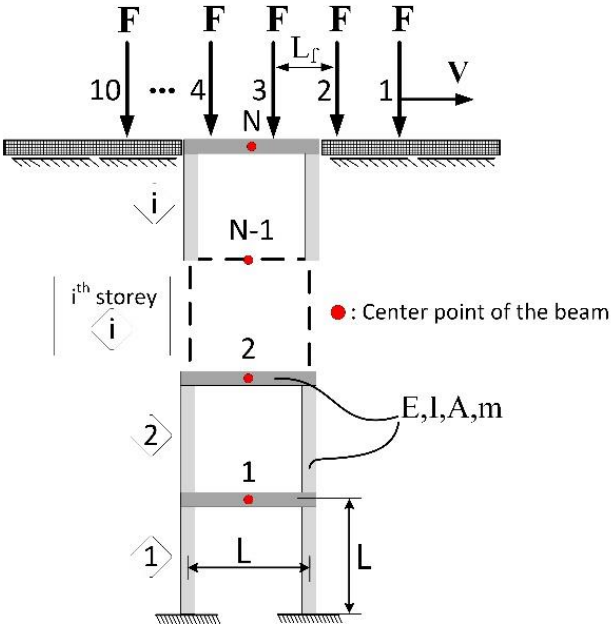

Fig. 1 A multi-storey frame subjected to moving train loads

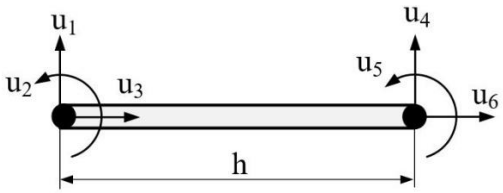

Fig. 2 6-DOF beam element

2.2 Finite element formulation

The Euler-Bernoulli beam element has two nodes and each node has three degrees of freedom (DOF), as shown in Fig. 2. The element mass and stiffness matrices can be found after applying standard finite element procedure.

The mass and stiffness matrices of the uniform beam element can be computed from

$$\mathbf{m}_b = m\int_0^h N_b(x/h)N_b(x/h)^T dx$$
$$\mathbf{k}_b = EI\int_0^h \mathbf{N}_b''(x/h)\mathbf{N}_b''(x/h)^T dx \tag{1}$$

for bending vibrations and

$$\mathbf{m}_a = m\int_0^h N_a(x/h)N_a(x/h)^T dx$$
$$\mathbf{k}_a = EA\int_0^h \mathbf{N}_a'(x/h)\mathbf{N}_a'(x/h)^T dx \tag{2}$$

for axial vibrations where E, I, m and h are elastic modulus, area moment of inertia, mass per unit length and beam length, respectively. Also, the prime sign represents derivative with respect to x.

N_b and N_a are the shape functions and are defined as follows (Meirovitch 1986)

$$\begin{gathered}\mathbf{N}_b = \left[N_{b1}\ N_{b2}\ N_{b3}\ N_{b4}\right]^T \\ N_{b1} = 1-3\xi^2+2\xi^3,\ \ N_{b2} = \xi-2\xi^2+\xi^3 \\ N_{b3} = 3\xi^2-2\xi^3,\ N_{b4} = -\xi^2+\xi^3\end{gathered} \tag{3}$$

$$\begin{gathered}\mathbf{N}_a = \left[N_{a1}\ N_{a2}\right]^T \\ N_{a1} = 1-\xi,\ \ N_{a2} = \xi\end{gathered} \tag{4}$$

where $\xi = x/h$.

The element mass (Eq. (1)) and stiffness (Eq. (2)) matrices are given by superposing the element matrices associated with the two-node elements

$$\mathbf{m}_e = \begin{bmatrix} m_b(1,1) & m_b(1,2) & 0 & m_b(1,3) & m_b(1,4) & 0 \\ m_b(2,1) & m_b(2,2) & 0 & m_b(2,3) & m_b(2,4) & 0 \\ 0 & 0 & m_a(1,1) & 0 & 0 & m_a(1,2) \\ m_b(3,1) & m_b(3,2) & 0 & m_b(3,3) & m_b(3,4) & 0 \\ m_b(4,1) & m_b(4,2) & 0 & m_b(4,3) & m_b(4,4) & 0 \\ 0 & 0 & m_a(2,1) & 0 & 0 & m_a(2,2) \end{bmatrix} \tag{5}$$

$$\mathbf{k}_e = \begin{bmatrix} k_b(1,1) & k_b(1,2) & 0 & k_b(1,3) & k_b(1,4) & 0 \\ k_b(2,1) & k_b(2,2) & 0 & k_b(2,3) & k_b(2,4) & 0 \\ 0 & 0 & k_a(1,1) & 0 & 0 & k_a(1,2) \\ k_b(3,1) & k_b(3,2) & 0 & k_b(3,3) & k_b(3,4) & 0 \\ k_b(4,1) & k_b(4,2) & 0 & k_b(4,3) & k_b(4,4) & 0 \\ 0 & 0 & k_a(2,1) & 0 & 0 & k_a(2,2) \end{bmatrix} \tag{6}$$

where $a(\mathrm{i},j)$ defines $(i,j)^{\mathrm{th}}$ element of matrix **a**.

To obtain the structural mass and stiffness matrices, considering the case of an element making an angle α with the U_3 axis (Fig. 3), the relation between local and global reference coordinates can be written as

$$\mathbf{T} = \begin{bmatrix} \mathbf{t} & \mathbf{0} \\ \mathbf{0} & \mathbf{t} \end{bmatrix} \tag{7}$$

and

$$\mathbf{t} = \begin{bmatrix} \cos\alpha & 0 & \cos(\pi/2+\alpha) \\ 0 & 1 & 0 \\ \cos(\pi/2-\alpha) & 0 & \cos\alpha \end{bmatrix} \tag{8}$$

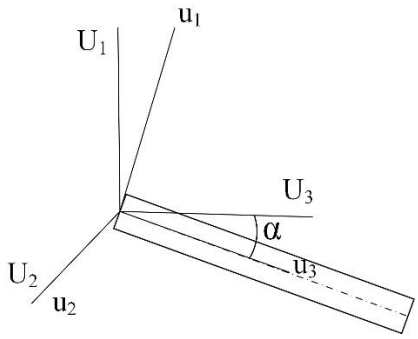

Fig. 3 $u_1u_2u_3$: Local coordinate system, $U_1U_2U_3$: Global coordinate system

where **T** is transformation matrix.

Mass and stiffness matrices of each element in local coordinate system should be transformed to global coordinate system

$$\mathbf{M_e} = \mathbf{T^T m_e T}, \quad \mathbf{K_e} = \mathbf{T^T k_e T} \tag{9}$$

where $\mathbf{m_e}$ and $\mathbf{k_e}$ are the respective mass and stiffness matrices in local coordinates. Also, $\mathbf{M_e}$ and $\mathbf{K_e}$ are element mass and stiffness matrices in global coordinates, respectively.

By assembling the element matrices, $\mathbf{M_e}$ and $\mathbf{K_e}$, equation of motion of multi-degree-of-freedom undamped structural system takes the form

$$\mathbf{M\,\ddot{U} + KU = F} \tag{10}$$

where **M** and **K** denote the overall global mass matrix and the overall global stiffness matrix, respectively. $\ddot{\mathbf{U}}$ and **U** are the respective acceleration and displacement vectors for the whole structure. **F** is the external time-dependent force vector.

To determine the equivalent forces at nodes, assume that the force F is on the s^{th} element of the beam. Then the equivalent force at nodes can be obtained as

$$f_i^{(j)}(i=1,.,6;\ j=1,.,n) = \begin{cases} & j=s & j\neq s \\ f_1^{(j)} & FN_{b1} & 0 \\ f_2^{(j)} & FN_{b2} & 0 \\ f_3^{(j)} & (0)N_{a1} & 0 \\ f_4^{(j)} & FN_{b3} & 0 \\ f_5^{(j)} & FN_{b4} & 0 \\ f_6^{(j)} & (0)N_{a2} & 0 \end{cases} \tag{11}$$

The Newmark integration method with parameters β and α were selected as β=0.25 and α=0.5 to obtain a stable solution (Bathe 1996).

3. Modal analysis of the multi-storey frame

Table 1 Physical and geometric properties of the multi-storey frame

Beam/column length (L), m	30
Force (F), N	60822
Elastic modulus (E), N/m^2	2.87e9
Area moment of inertia (I), m^4	2.9
Cross-section area (A), m^2	8.7
Mass per unit length (m), kg/m	2303
Element size, m	5

Table 2 The first few natural frequencies of i-storey frame (i=1,2,3,4)

f(Hz)	1-storey		2-storey		3-storey		4-storey	
	Present Work	ANSYS	Present Work	ANSYS	Present Work	ANSYS	Present Work	ANSYS
f_1	1.0762	1.0760	0.5020	0.5020	0.3176	0.3176	0.2307	0.2307
f_2	4.2178	4.2100	1.6503	1.6493	1.0518	1.0515	0.7479	0.7478
f_3			3.6168	3.6102	1.9017	1.9004	1.3843	1.3837
f_4			4.9873	4.9784	3.4572	3.4510	2.0335	2.0320
f_5					4.3706	4.3626	3.3939	3.3878
f_6							3.9822	3.9752
f_7							4.4549	4.4511

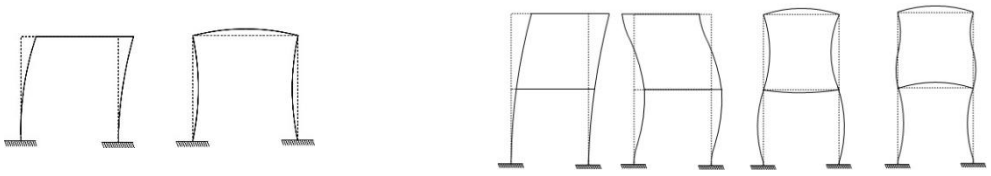

(a) 1-storey frame 2-storey frame

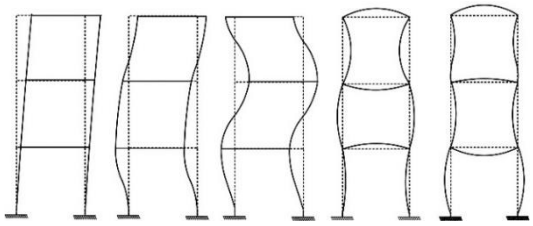

(c) 3-storey frame

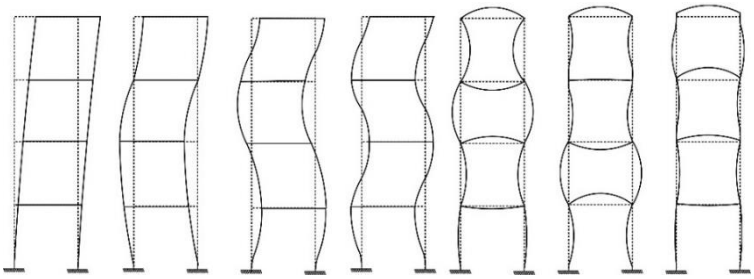

(d) 4-storey frame

Fig. 4 The first few mode shapes of i-storey frame (i=1,2,3,4). The modes corresponding to the natural frequencies listed in Table 2 are given in increasing order from left to right

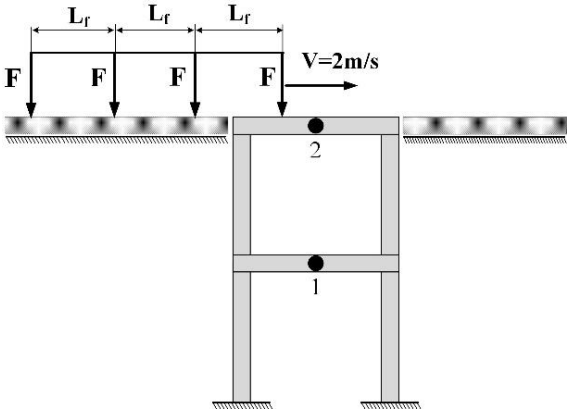

Fig. 5 2-storey frame under moving loads

All the parameters which are used in subsequent computations have been given in Table 1. The values of physical properties are taken from Ref. (Yang *et al.* 1997).

The first few natural frequencies are determined using both ANSYS and the developed MATLAB programs (present work). The beams and columns are modelled using BEAM54 element. ANSYS BEAM54 is used because it has the same nodal degrees of freedom with the model developed by present work. Element size is taken as 5 m to generate the same finite element mesh those of the developed model. Table 2 shows the natural frequencies of *i*-storey frame (i=1,2,3,4).

The mode shapes for those natural frequencies given in Table 2 is determined. The first modes of the structure shown in Figs. 4 (a)-(d) correspond to the first bending modes of the columns forming the frame. The displacement of the beam in the vertical direction has become important in the second mode of the 1-storey frame. This mode corresponds to the first mode in which the vertical direction of the beam is effective. Therefore, the natural frequency of the structure in this mode is shown in Table 2 with a dark background. The 2nd mode of the 2, 3 and 4-storey frames corresponds to the 2nd bending mode of the columns. The 3rd mode of the 3 and 4-storey frame corresponds to the 3rd bending mode of the columns. Finally, the 4th mode of the 4-storey frame corresponds to the 4th bending mode of the columns. The displacement of the top beam in the vertical direction is negligible in the above-mentioned modes.

In this study, the load moves on the top beam of the structure. The study will be limited to the vertical vibrations of the structure. Therefore, the displacements of the top beam in the vertical direction are important in the resonance behaviour of the structure under the influence of the successive moving loads. Hence, the 2nd mode for the 1-storey frame, the 3rd or 4th mode of the 2-storey frame, the 4th or 5th mode of the 3-storey frame and the 5th, 6th or 7th mode of the 4-storey frame can be expected to be dominant in the resonance behavior.

4. Effect of mode shape on the dynamic response

It is known that structures vibrate under resonance conditions in certain situations due to the passage of repeated groups of loads. The load velocity and force span length are important parameters on the resonance vibrations. The resonance vibrations can be observed in some values of these parameters.

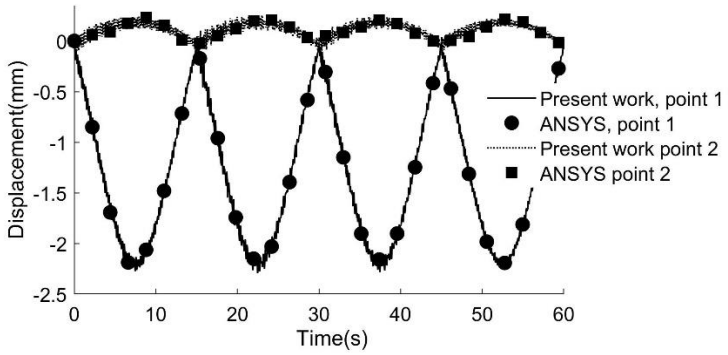

Fig. 6 Vertical deflections at points 1 and 2

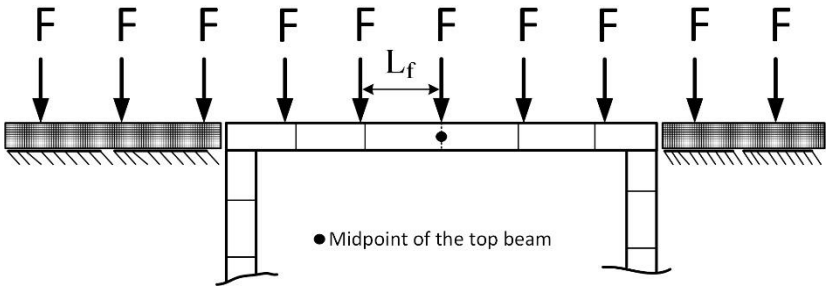

Fig. 7 Calculation of the maximum static deflection at midpoint of the top beam

4.1 Validation

To prove the validity of the finite element model (present work), it is reasonable to compare the results with those of ANSYS software. The loads consist in a succession of 4 concentrated moving loads of constant intervals L_f=30 m travelling at constant speed V=2 m/s (see Fig. 5).

The vertical vibration response for center points 1 and 2 of the 2-storey frame are shown in Fig. 6. The time delay of successive forces is the same and its value equals L_f/V=15 s. Because of beam length $L=L_f$, the displacement/time plot, given in Fig. 6, has four peaks. Very good agreement is observed.

4.2 Velocity-foce span length to beam length ratio-dynamic magnification factor

A i-storey frame (i=1,2,3,4) subjected to successive moving forces with constant interval (Fig. 1) is considered here. The effect of velocity and force span length on the dynamic response was investigated by plotting the velocity (V) - force span length to beam length ratio ($\bar{L}$) - dynamic magnification factor (DMF) plot. The DMF is defined as the ratio of the maximum dynamic deflection to the maximum static deflection. The maximum static deflection is computed at the midpoint of the top beam, as shown in Fig. 7. The static forces were defined in such a way that one of the forces was applied at the center of the beam.

Fig. 8 shows 3D views of V-$\bar{L}$-DMF plot of 1-storey frame. Three typical points (P_1, P_2 and P_3)

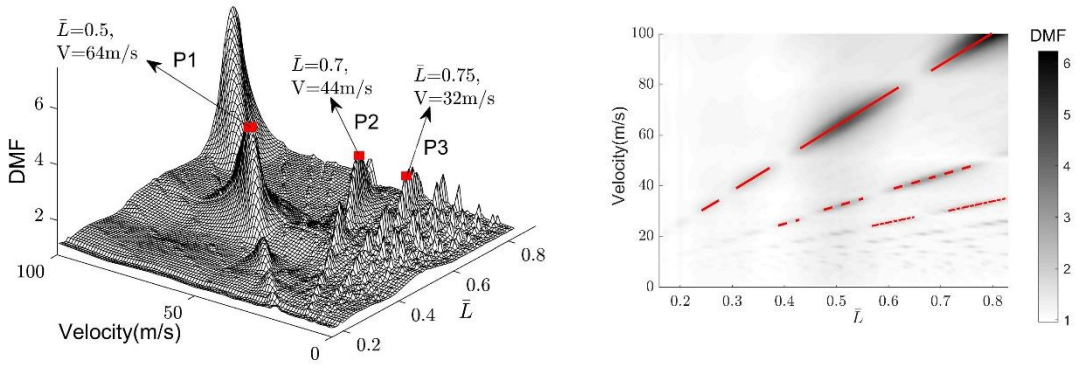

(a) (b)

Fig. 8 1-storey frame, (a) *V*-$\bar{L}$-*DMF* plot, (b) its 2D projection

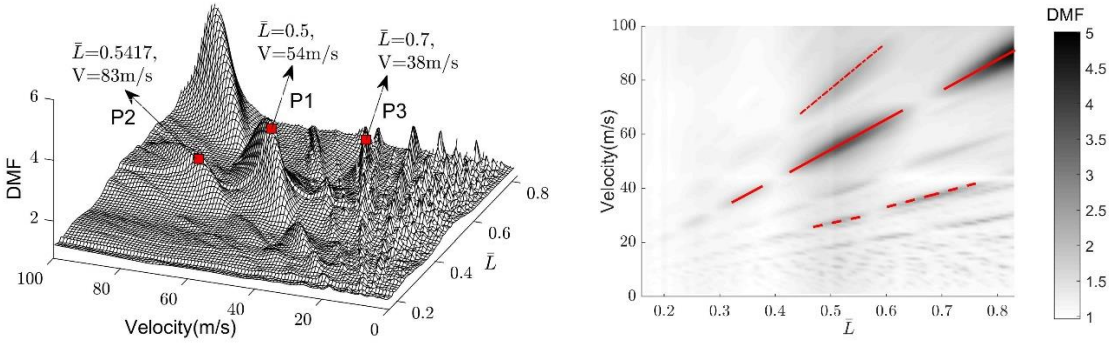

(a) (b)

Fig. 9 2-storey frame, (a) *V*-$\bar{L}$-*DMF* plot, (b) its 2D projection

that correspond to the maximum *DMF* are selected. The values *V*=64 m/s, $\bar{L}$=0.5; *V*=44 m/s, $\bar{L}$=0.7; and *V*=32 m/s, $\bar{L}$=0.75 are read from these three points, respectively.

The maximum DMF values of the 3D *V*-$\bar{L}$-*DMF* curves shown in Figs. 8(a)-11(a) depend on $\bar{L}$ and *V*. If $\bar{L}$ changes the specific velocity (critical velocity, V_{cr}), which causes the largest maximum displacement also changes. As can be seen in Figs. 8 (b)-10 (b), the variation of V_{cr} with $\bar{L}$ is linear. Figs. 8(b)-10(b) provide directions corresponding to critical speeds. The most important of these directions is the solid line because it gives the largest maximum DMF values. Fig. 8(b) shows that the other two directions are below the solid line.

Fig. 9 illustrates 3D *V*-$\bar{L}$-*DMF* plot of 2-storey frame. The points P_1, P_2 and P_3 have values of *V*=54 m/s, $\bar{L}$=0.5; *V*=83 m/s, $\bar{L}$=0.5417; and *V*=38 m/s, $\bar{L}$=0.7, respectively. Fig. 9(b) is a two-dimensional representation of Fig. 9(a). Here the color bar shows *DMF*. The three directions corresponding to the critical speed are shown in this figure. From these directions, the dashed-dotted line is above the solid line and the dashed line is below.

The 3D *V*-$\bar{L}$-*DMF* is plotted for the 3-storey frame, as shown in Fig. 10. The three points selected on this figure are as follows: *V*=51 m/s, $\bar{L}$=0.5 at point P_1; *V*=71 m/s, $\bar{L}$=0.5417 at point P_2; and *V*=38 m/s, $\bar{L}$=0.7 at point P_3. Fig. 10(b) shows the directions giving critical speeds. It is observed

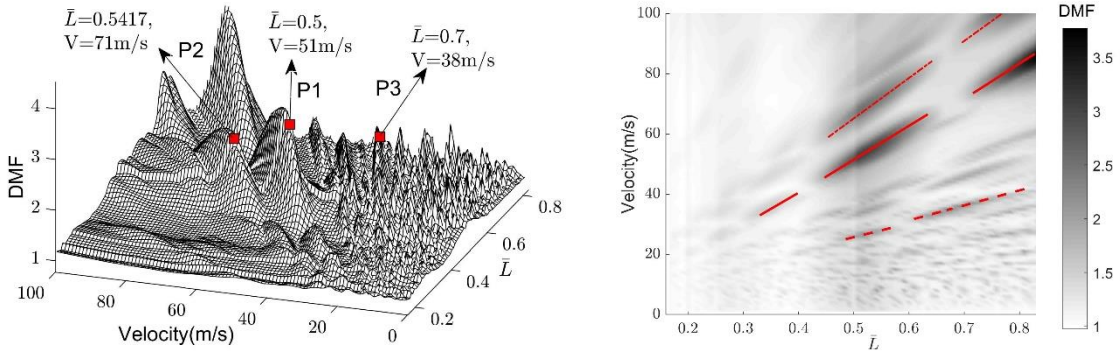

(a) (b)

Fig. 10 3-storey frame, (a) *V*-$\bar{L}$-*DMF* plot, (b) its 2D projection

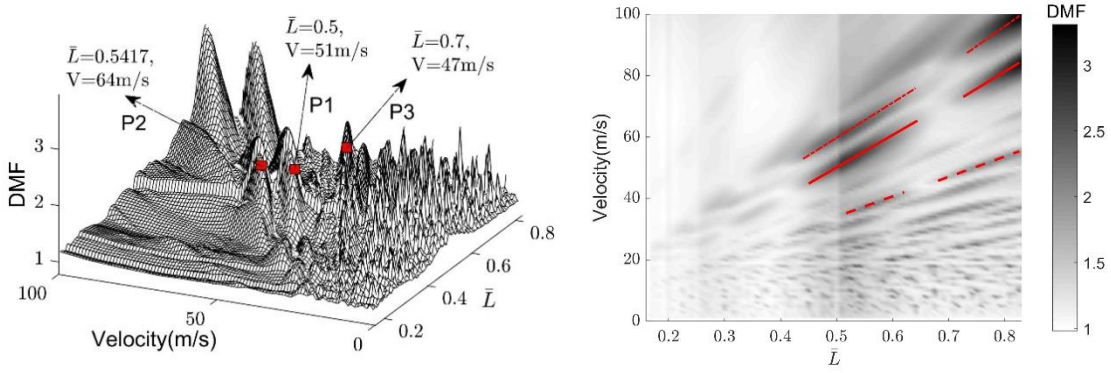

(a) (b)

Fig. 11 4-storey frame, (a) *V*-$\bar{L}$-*DMF* plot, (b) its 2D projection

that the solid line and dashed-dotted line approaching each other when compared to the case of the 2-storey frame.

From Fig. 11(a), the points P_1, P_2 and P_3 for the 4-storey frame are taken as V=51 m/s, $\bar{L}$=0.5; V=64 m/s, $\bar{L}$=0.5417; and V=47 m/s, $\bar{L}$=0.7, respectively. As a result of the increase of storey number of the structure, the difference between the consecutive natural frequencies of the structure decreased. Therefore, as seen in Fig. 11(b) the dashed-dotted line and the solid line are getting closer to each other.

4.3 Time and frequency response

To show which mode is dominating the dynamic responses of multi-storey frames, the Fourier transform of the free response is calculated. The graphs are plotted for the three points indicated in Section 4.2 for each frame. The graphs plotted below are the displacements (or frequency) in the vertical direction of the point N (see also 1) for the N-storey frame. It is selected due to the maximum displacement are expected to occur at this point when the structure is subjected to moving train loads.

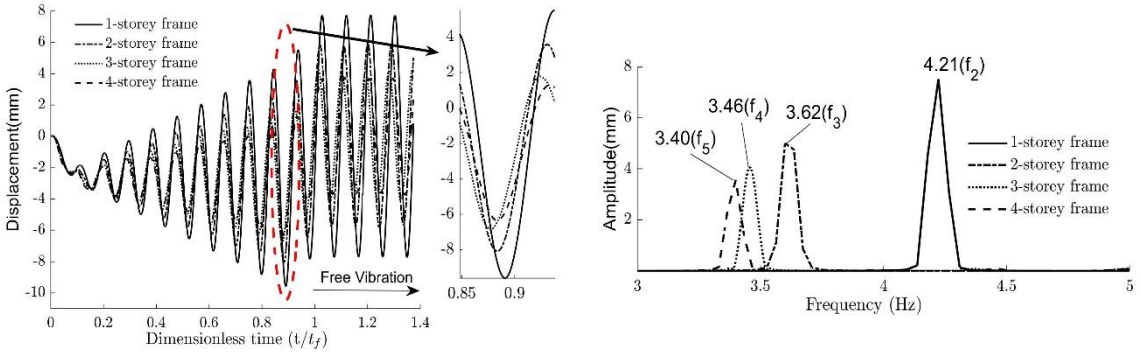

(a) (b)

Fig. 12 (a) Time history curves of free and forced response at point P_1, (b) frequency response

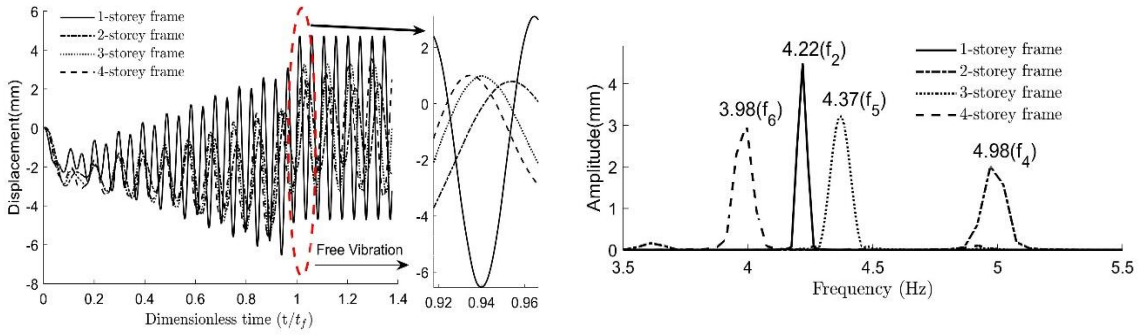

(a) (b)

Fig. 13 (a) Time history curves of free and forced response at point P_2, (b) frequency response

Fig. 12(a) shows the time history graphs for the V and $\bar{L}$ values at the point P_1 of the i-storey frame (i=1,2,3,4). Here, the t_f in the dimensionless time axis indicates the time that the load leaves the structure. It is clear that the values t/t_f greater than 1 illustrate free vibrations. By taking the Fourier transform of the free vibration responses, the frequency responses, as shown in Fig. 12(b), were obtained.

In Fig. 12(b), it is seen that the values taken from point P_1 for 1-storey frame excite the 2nd mode of vibration with the natural frequency of 4.21 Hz. A similar situation can be said to be the 3rd mode of the 2-storey frame, the 4th mode of the 3-storey frame and the 5th mode of the 4-storey frame. Furthermore, if P_1 is considered to be a point on the solid line shown in Figs. 8(b)-11(b), it can be concluded that the points taken on the solid line will again excite the same modes.

Fig. 13(a) depicts displacements against dimensionless time plots for those values taken at point P_2 of the i-storey frame (i=1,2,3,4). From Fig. 13(b), as in P_1, the 2nd mode of the 1-storey frame dominates the resonance response. In contrast, the 4th mode of the 2-storey frame, the 5th mode of the 3-storey frame, and the 6th mode of the 4-storey frame are excited at this point. Also, this point is a typical point taken on the dashed line in Figs. 8(b)-11(b). Note that these dashed lines for the 1-storey frames are below the solid line, while they are above the solid line for 2-4 storey frames.

Fig. 14(a) shows the time history and frequency response plots for the values picked at point P_3.

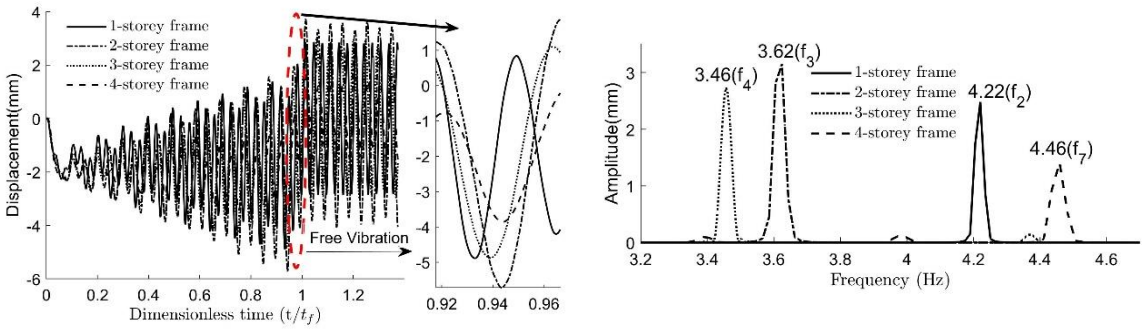

(a) (b)

Fig. 14 (a) Time history curves of free and forced response at point P_3, (b) frequency response

For the 1, 2 and 3-storey frames, just like point P_1, the excited modes are the 2nd, 3rd and 4th modes, respectively (Fig. 14(b)). However, the resonance response of the 4-storey frame seems to be related to the 7th mode of the structure. These modes are effective in the resonance response of the structures at a value from any point on the dashed-dotted line in Fig. 11(b). The flexibility of the structure increases with the increase in storey number. This means that higher modes may affect the resonance response, depending on the mode shape of the structure.

5. Conclusions

In this study, it has been investigated which mode shapes are effective in the resonance response of a multi-storey frame. The analyses are restricted by the vibrations in the vertical direction under the moving load sequence of the structure. The beams and columns forming the structure are modelled by Euler-Bernoulli beam theory. The graphs are plotted for the midpoint of the top beam on which the load moves. First, natural frequencies and mode shapes of the structure are determined. Then, the effect of the velocity of the moving load sequence and the load-span / beam length ratio on the DMF is determined by using the 3D *V-L̄-DMF* plots and its 2D projections. Three typical points are selected from 3D graphics. Furthermore, these points are on the three basic directions seen in the 2D graph corresponding to the critical speeds. Last, time history and frequency responses are obtained at these points. It has been determined which mode is excited in the specified directions. The followings are the conclusions made from this study:

- The resonance response of the multi-storey frame takes place in one of the mode shapes where the displacement of the top beam in the vertical direction is significant.
- Large DMF values are obtained in the first mode where the displacement of the top beam was significant. These mode shapes were determined as 2nd mode for the 1-storey frame, 3rd mode for the 2-storey frame, 4th mode for the 3-storey frame and 5th mode for the 4-storey frame. This leads to result that if the storey number of the structure is N, the effect of N+1th mode on the resonance response should be taken into account.
- The increase in the storey number of the structure has also increased the effects of the higher modes on the DMF. For example, the effects of the 5th and 6th modes on dynamic response are close to each other in the 4-storey frame.

References

Bathe, K.J. (1996), *Finite Element Procedures*, Prentice Hall, New Jersey, USA.

Fu, C. (2015), "The effect of switching cracks on the vibration of a continuous beam bridge subjected to moving vehicles", *J. Sound Vib.*, **339**, 157-175. https://doi.org/10.1016/j.jsv.2014.11.009.

Kiral, Z. and Kiral, B.G. (2007), "Dynamic analysis of a symmetric laminated composite beam subjected to a moving load with constant velocity", *J. Reinf. Plast. Compos.*, **27**(1), 19-32. https://doi.org/10.1177/0731684407079492.

Koziol, P. (2016), "Experimental validation of wavelet based solution for dynamic response of railway track subjected to a moving train", *Mech. Syst. Signal Pr.*, **79**, 174-181. https://doi.org/10.1016/j.ymssp.2016.02.058.

Meirovitch, L. (1986), *Elements of Vibration Analysis*, McGraw-Hill, New York, USA.

Mohebpour, S.R., Vaghefi, M. and Ezzati, M. (2016), "Numerical analysis of an inclined cross-ply laminated composite beam subjected to moving mass with consideration the Coriolis and centrifugal forces", *Eur. J. Mech., A/Solid.*, **59**, 67-75. https://doi.org/10.1016/j.euromechsol.2016.03.003.

Ozturk, H., Yashar, A. and Sabuncu, M. (2015), "Dynamic stability of cracked multi-bay frame structures", *Mech. Adv. Mater. Struct.*, **23**(6), 715-726. https://doi.org/10.1080/15376494.2015.1029160.

Song, Y., Kim, T. and Lee, U. (2016), "Vibration of a beam subjected to a moving force: Frequency-domain spectral element modeling and analysis", *Int. J. Mech. Sci.*, **113**, 162-174. https://doi.org/10.1016/j.ijmecsci.2016.04.020.

Svedholm, C., Zangeneh, A., Pacoste, C., Franćois, S. and Karoumi, R. (2016), "Vibration of damped uniform beams with general end conditions under moving loads", *Eng. Struct.*, **126**, 40-52. https://doi.org/10.1016/j.engstruct.2016.07.037.

Thambiratnam, D. and Zhuge, Y. (1996), "Dynamic analysis of beams on an elastic foundation subjected to moving loads", *J. Sound Vib.*, **198**(2), 149-169. https://doi.org/10.1006/jsvi.1996.0562.

Wu, J.J., Whittaker, A. and Cartmell, M. (2000), "The use of finite element techniques for calculating the dynamic response of structures to moving loads", *Comput. Struct.*, **78**(6), 789-799. https://doi.org/http://dx.doi.org/10.1016/S0045-7949(00)00055-9.

Wu, J.J., Whittaker, A. and Cartmell, M. (2001), "Dynamic responses of structures to moving bodies using combined finite element and analytical methods", *Int. J. Mech. Sci.*, **43**, 2555-2579. https://doi.org/10.1016/S0020-7403(01)00054-6.

Yang, Y.B., Yau, J.D. and Hsu, L.C. (1997), "Vibration of simple beams due to trains moving at high speeds", *Eng. Struct.*, **19**(11), 936-944. https://doi.org/http://dx.doi.org/10.1016/S0141-0296(97)00001-1.fdxf.

Yang, Y.B., Lin, C.L., Yau, J.D. and Chang, D.W. (2004), "Mechanism of resonance and cancellation for train-induced vibrations on bridges with elastic bearings", *J. Sound Vib.*, **269**, 345-360. https://doi.org/10.1016/S0022-460X(03)00123-8.

Zrnić, N.D., Gašić, V.M. and Bošnjak, S.M. (2015), "Dynamic responses of a gantry crane system due to a moving body considered as moving oscillator", *Arch. Civil Mech. Eng.*, **15**(1), 243-250. https://doi.org/10.1016/j.acme.2014.02.002.